



HAL
open science

Krit 1 interactions with microtubules and membranes are regulated by Rap1 and integrin cytoplasmic domain associated protein-1.

Sophie Béraud-Dufour, Romain Gautier, Corinne Albiges-Rizo, Pierre Chardin, Eva Faurobert

► **To cite this version:**

Sophie Béraud-Dufour, Romain Gautier, Corinne Albiges-Rizo, Pierre Chardin, Eva Faurobert. Krit 1 interactions with microtubules and membranes are regulated by Rap1 and integrin cytoplasmic domain associated protein-1.. FEBS Journal, 2007, 274 (21), pp.5518-32. 10.1111/j.1742-4658.2007.06068.x . inserm-00322435

HAL Id: inserm-00322435

<https://inserm.hal.science/inserm-00322435>

Submitted on 3 Oct 2008

HAL is a multi-disciplinary open access archive for the deposit and dissemination of scientific research documents, whether they are published or not. The documents may come from teaching and research institutions in France or abroad, or from public or private research centers.

L'archive ouverte pluridisciplinaire **HAL**, est destinée au dépôt et à la diffusion de documents scientifiques de niveau recherche, publiés ou non, émanant des établissements d'enseignement et de recherche français ou étrangers, des laboratoires publics ou privés.

Krit1 interactions with microtubules and membranes are regulated by Rap1 and ICAP-1.

Sophie Béraud-Dufour, Romain Gautier, Corinne Albiges-Rizo*, Pierre Chardin and Eva Faurobert.

UMR 6097 CNRS-UNSA, Institut de Pharmacologie Moléculaire et Cellulaire, 660 route des lucioles, 06560 Vabonne, France, * CRI U823 Université Joseph Fourier, Institut Albert Bonniot équipe 1 DYSAD, Site Santé La Tronche, 38042 Grenoble, France.

Address correspondence to: Eva Faurobert, CRI U823 Université Joseph Fourier, Institut Albert Bonniot équipe 1 DYSAD, Site Santé La Tronche BP170, 38042 Grenoble CEDEX 9, France
Tel: 00-33-476-54-94-74; Fax: 00-33-476-54-94-25; E-Mail: faurobert@ipmc.cnrs.fr

Short title: Rap1 regulates Krit1 microtubule and lipid binding

ABSTRACT

The small G protein Rap1 regulates diverse cellular processes such as integrin activation, cell adhesion, cell-cell junction formation and cell polarity. It is crucial to identify Rap1 effectors to better understand signalling pathways controlling these processes. Krit1, a FERM protein, was identified as a Rap1 partner in a yeast two-hybrid screen, but this interaction was not confirmed in subsequent studies. As evidence suggests a role for Krit1 in Rap1-dependent pathways, we readdressed this question. Here, we demonstrate by biochemical assays that Krit1 is a specific Rap1 effector. We show that, like other FERM proteins, Krit1 adopts two conformations: a closed conformation in which its N-terminal NPAY motif interacts with its C-terminus and an opened conformation bound to ICAP-1, a negative regulator of focal adhesion assembly. We show that a ternary complex can form in vitro between Krit1, Rap1 and ICAP-1 and that Rap1 binds Krit1 FERM domain in both closed and opened conformations. Unlike ICAP-1, Rap1 does not open Krit1. Using sedimentation assays, we show that Krit1 binds in vitro to microtubules through its N and C-termini and that Rap1 and ICAP-1 inhibit Krit1 binding to microtubules. Consistently, YFP-Krit1 localizes on CFP-labelled microtubules in BHK cells and is delocalized from microtubules upon co-expression with activated Rap1V12. Finally, we show that Krit1 binds to PIP₂ containing liposomes and that Rap1 enhances this binding. Based on these results, we propose a model in which Krit1 would be delivered by microtubules to the plasma membrane where it would be captured by Rap1 and ICAP-1.

Keywords: Rap1, Krit1, CCM1, FERM domain, PTB, microtubules, PIP₂

The abbreviations used are: MT: microtubules, Krit1: Krev Interaction Trapped gene, CCM1: cerebral cavernous malformation 1, ICAP-1: Integrin Cytoplasmic Domain Associated Protein, PTB: Phosphotyrosine-binding domain, FERM: band Four-point-one/Ezrin/Radixin/Moesin

INTRODUCTION

The small G protein Rap1 (Krev-1), a member of the Ras superfamily, has been brought to the forefront since the discovery that it regulates diverse cellular processes such as integrin activation and cell adhesion, cell spreading, cell polarity and cell-cell junction formation [1],[2],[3]. To gain more insights into these pathways, a variety of effector proteins that interact with active Rap1GTP-bound form has been identified. Among them, RAPL, which is enriched in lymphoid tissues, activates the integrin α L β 2, most likely by interacting with α L integrin [4] and RIAM, which binds to different actin regulators, participates in an integrin activation complex that binds to and activates β integrins [5]. VAV1 and TIAM1 are localized by Rap1GTP to sites of cell spreading and serve as exchange factors for Rac [6]. ARAP3 is a GTPase-activating protein for RhoA and Arf6 that affects PDGF-induced lamellipodia formation [7]. In dictyostelium, Phg2 promotes myosin II disassembly at the front of chemotaxing cell facilitating filamentous-actin mediated leading edge protrusion [8]. Afadin/AF6 participates in the maturation of cell-cell junctions [9].

Krit1 (Krev Interaction Trapped gene) was identified in 1997 as a Rap1 partner in a yeast two-hybrid screen [10], but subsequent studies did not confirm their interaction [11], leading to the conclusion that Krit1 is not a Rap1 partner [12]. However, several pieces of evidence concerning a potential role of Krit1 in Rap1-regulated cellular processes prompted us to reconsider this question. First, it has recently been demonstrated that Rap1-dependent activation of integrins requires talin binding to the cytoplasmic tail of β integrin [13]. Talin is an essential integrin-activating protein that connects the cytoplasmic tail of β integrins to the actin cytoskeleton [14]. ICAP-1 (Integrin Cytoplasmic Domain Associated Protein) is a partner of the cytoplasmic tail of β 1 integrin and it has been shown to compete with talin for binding to β 1 integrin [15]. Consistently, on ICAP-1-null osteoblasts and fibroblasts, fibronectin receptors are in an active conformation and β 1-dependent cell adhesion is enhanced compared to that of wild-type cells [16],[17]. On the opposite, overexpression of ICAP-1 reduces cell spreading and disorganizes focal adhesions [15]. These results suggest that at resting state, β 1 integrin is kept inactive through binding of ICAP-1 to its cytoplasmic tail. Interestingly, Krit1 is a partner of ICAP-1 [11], [18]. Yeast-two hybrid studies have shown that Krit1 competes with β 1 integrin for binding to ICAP-1 [11], suggesting that Krit1 could relieve the inhibitory effect of ICAP-1 on β 1 integrin

activation. The second piece of evidence concerns the existence of a human genetic disease linked to mutations in Krit1 gene. CCM1 (cerebral cavernous malformation 1) corresponds to brain capillaries malformations characterized by clusters of dilated thin-walled blood vessels [19]. These lesions usually hemorrhage resulting in seizures, focal neurological deficits or stroke. Ultrastructural studies show that tight junctions are absent between the endothelial cells in these lesions and that the surrounding basal lamina is hypertrophied [20].

Very little is known about the Krit1 protein and its subcellular localization. First, Krit1 C-terminus amino acid sequence bears homologies with FERM domains (present in band Four-point-one/Ezrin/Radixin/Moesin). FERM domains localize proteins to the plasma membrane, where they can interact with phosphoinositides and membrane proteins [21]. The FERM domain of talin interacts with phosphatidylinositol 4, 5-P₂ (PIP₂) and with the cytoplasmic tail of β integrins [14]. Moreover, proteins with FERM domains usually exist in two conformational states: a closed “inactive” conformation where the FERM domain is masked by another part of the protein and an open “active” conformation where the FERM domain is unmasked. Cleavage, phosphorylation or (PIP₂) binding are activation signals [21]. Second, it has been reported that Krit1 interacts with tubulin in BAEC and decorates microtubules all along their length [22]. However, this interaction has been questioned because the antibody used in this study recognized a protein of lower size on western blot. Another antibody has since identified a protein of the predicted size, but the primary location of Krit1 awaits elucidation [39]. Since microtubules are known to regulate the dynamics of focal adhesion assembly [23],[24], we readressed this important issue.

In this paper, we sought for the interaction of Krit1 with Rap1, microtubules and membranes. We show that Krit1, like many proteins with FERM domains, adopts a closed conformation. This closed conformation is opened by ICAP-1. Importantly, we confirm that Krit1 interacts specifically with Rap1 and preferentially with active Rap1 (GTP-bound form), ending the debate about this point. We show that Rap1 binds to the FERM domain of Krit1 both in its closed and opened conformations and that, unlike ICAP-1, Rap1 does not open Krit1. Moreover, we demonstrate that Krit1, Rap1 and ICAP-1 can form a ternary complex in vitro. We show that Krit1 interacts with in vitro polymerized microtubules, and with PIP₂ on artificial membranes. Remarkably, we demonstrate that Rap1 and ICAP-1 inhibit in vitro Krit1 binding to microtubules and that Rap1 stimulates Krit1 binding to membranes. Consistently, YFP-Krit1

localizes on CFP-labelled microtubules in BHK cells and is delocalized from microtubules upon co-expression with activated Rap1.

RESULTS

Krit1 contains a putative FERM domain and binds to PIP₂

Tri-dimensional structure of the FERM domain of the archetypal ERM proteins, ezrin, radixin and moesin, have been resolved by crystallography [25],[26],[27]. They are composed of three sub-domains F1 to F3 arranged in a clover-shaped fashion (Fig. 1A). F3 sub-domain resembles a PTB domain, a conserved structural fold that binds to protein NPxY motifs [28]. Analysis of Krit1 sequence using Blast program shows that the last 300 amino acid residues of Krit1 bear roughly 20% identity with F1, F2, F3 sub-domains of the typical ERM proteins (ezrin, radixin, moesin, talin). Even though this is the lower limit for comparative modelling, we were able to generate models for Krit1 F1 and F2-F3 sub-domains structure based on the homology with radixin F1 in complex with IP3 and with talin F2-F3. (Fig. 1B). These models displayed very stable secondary structures and energies throughout molecular dynamics simulations, strongly supporting the idea that Krit1 C-terminus folds as a FERM domain.

A functional feature of FERM domains is their capacity to interact with PIP₂ on plasma membrane. In the radixin-IP3 co-crystal, IP3 binds to a basic cleft located between F1 and F3 sub-domains and folded around a tryptophan present at the hydrophobic base of the cleft [26] (Fig. 1A). Interestingly, on our model of the Krit1 FERM domain, basic residues are also found in the cleft between sub-domain F1 and F3 and the tryptophan at the base of the pocket is conserved (Fig. 1B), implying that Krit1 would have the structural features required for binding to phospho-inositides on membranes. We therefore tested the ability of Krit1 to binding to PIP₂ containing membranes. Krit1 was incubated with artificial liposomes supplemented or not with 2% PIP₂ at increasing NaCl concentrations. At 100 mM NaCl, 70 % of Krit1 bound to PIP₂ containing liposomes, whereas less than 10% bound to liposomes without PIP₂, showing that Krit1 interacts mainly with PIP₂ on these liposomes (Fig. 1C). Moreover, increasing salt concentrations decreased Krit1 binding, highlighting the electrostatic status of this interaction (Fig. 1C).

Krit1 exists in a closed conformation opened by ICAP-1.

Intriguingly, in addition to its C-terminal FERM domain, Krit1 has a NPAY motif on its N-terminus that binds to ICAP-1 [11], [18]. This peculiarity of Krit1 led us to ask whether this motif could interact with Krit1 F3 PTB-like sub-domain. To test this hypothesis, we separately expressed His-tagged N-terminus (1 to 207 aa) and GST-C-terminus (207-end), which we called Krit1-NTer and GST-HypoKrit1, respectively (Fig. 2A). GST pull-down assays were performed by mixing these two fragments at a concentration of 100 nM each. Remarkably, Krit1-NTer bound specifically to GST-HypoKrit1 and to GST-ICAP-1 used as a positive control, but it did not bind to GST alone (Fig. 2B). To test whether the NPAY motif is involved in this interaction, we mutated Asn192 and Tyr195 into alanines in Krit1-NTer (Fig. 2A). Krit1-NTer APAA mutant did not interact with GST-HypoKrit1 and interacted only very weakly with GST-ICAP-1 as previously reported [11] (Fig. 2B). In an other assay, ICAP-1 totally prevented the binding of Krit1-NTer (5 μ M) to GST-HypoKrit1 (3.5 μ M) when added at equimolar concentration with Krit1-Nter (Fig. 2C), which correlates well with the observation that ICAP-1 had a better affinity for Krit1-Nter than HypoKrit1 (Fig. 2B).

These results show that Krit1 C-terminal FERM domain interacts with Krit1 N-terminus in vitro, and that this interaction requires the ICAP-1 binding motif NPAY. They suggest that full-length Krit1 exists in a closed conformation with the N-terminus folded on the C-terminus and that ICAP-1 binding to the N-terminal part disrupts Krit1 N and C-termini interaction.

Krit1 interacts with Rap1 preferentially in its GTP γ S bound form.

To answer the question of whether Krit1 is a Rap1 effector, i. e. whether Krit1 interacts preferentially with Rap1 in its GTP-bound form, we performed GST-pull down assays. Since we could not purify GST-full-length Krit1 because of its insolubility in E.Coli, we studied the binding of Rap1 to GST-HypoKrit1. We compared the binding of 1 μ M of Rap1 loaded with GDP or GTP γ S to 10 μ M of GST-HypoKrit1 by GST pull-down experiments. Unless specified, all the experiments were performed with Rap1A isoform. Rap1 binding to HypoKrit1 was specific, as no binding was observed to GST. Rap1GTP γ S bound twice more strongly to HypoKrit1 than did Rap1GDP, reflecting a higher affinity of active Rap1 for HypoKrit1 (Fig. 3A). In the same assay conditions, H-Ras GTP γ S did not bind to HypoKrit1 (Fig. 3A). This experiment therefore shows that Krit1 is a specific effector of Rap1.

Rap1 binds to the C-terminus of Krit1.

Serebriiskii et al. mapped a binding site for Rap1 in the 50 last a.a residues of the N-truncated form of Krit1 that they originally identified [10]. To verify this result, this site was deleted in GST-HypoKrit1 (Fig 2A). The resulting GST-HypoKrit1 Δ C mutant has a truncation of half of its F3 subdomain. We used the same experimental conditions as in figure 3A. Deletion of the C-terminus of Krit1 abolished the binding of Rap1GTP γ S to GST-HypoKrit1 (Fig. 3B), confirming that Rap1 binds to Krit1 C-terminal FERM domain.

Krit1, Rap1, and ICAP-1 form a ternary complex in vitro.

Since Krit1 can interact independently with ICAP-1 and with Rap1, we tested whether a ternary complex can form between the three proteins. We purified His-tagged full-length Krit1 from E. Coli and we performed GST pull-downs by mixing full-length Krit1 with Rap1GTP γ S and GST-ICAP-1 at a final concentration of 5 μ M each (Fig. 4). Krit1 interacted specifically with GST-ICAP-1 and not with GST alone. This interaction was strong enough to be revealed by staining of the proteins with Sypro Orange. As expected, Rap1GTP γ S did not interact with GST-ICAP-1. Interestingly, when Krit1 and Rap1GTP γ S were added together, Rap1GTP γ S was pulled-down with Krit1 on GST-ICAP-1 beads. Immunoblotting of Rap1 was necessary to reveal Rap1 binding, indicative of a weaker interaction of Krit1 with Rap1 than with ICAP-1. Therefore, this experiment shows that the three proteins form a ternary complex in vitro.

Rap1 binds equally to Krit1 opened and closed conformations and does not open Krit1.

Next, we compared the binding of Rap1 to Krit1 closed and opened conformations. To do so, we measured by GST-pull down the binding of 10 μ M of Rap1 GTP γ S on 3 μ M of GST-HypoKrit1 beads in absence or presence of 10 μ M of Krit1-NTer. Importantly, Krit1-NTer binding to GST-HypoKrit1 did not affect the interaction of Rap1GTP γ S to GST-HypoKrit1 (Fig. 5A). Conversely, Rap1 did not modify the binding of Krit1-NTer to HypoKrit1, suggesting that Rap1 binds to Krit1 closed conformation and does not open it. Moreover, the binding of Rap1GTP γ S to GST-HypoKrit1 was not modified either when the complex between HypoKrit1 and Krit1-NTer was disrupted by the addition of 10 μ M of ICAP-1, implying that the opening of Krit1 by ICAP-1 does not affect Rap1 binding (Fig. 5A). This result was confirmed on full length Krit1

by FLAG-pull-down experiment using FLAG-tagged Krit1. Addition of ICAP-1 together with Rap1 did not change Rap1 binding to Krit1 (Fig. 5B). Therefore, Rap1 and ICAP-1 can bind independently to Krit1. All together, our results suggest that, unlike ICAP-1, Rap1 binding to the C-terminal FERM domain does not induce the opening of Krit1 and that Rap1 binds as well on Krit1 closed and opened conformations (Fig. 5C).

Krit1 interacts in vitro with microtubules via two sites present respectively on its N- and C-termini.

It has previously been shown that Krit1 colocalizes with microtubules in BAEC [22]. However, the antibody used in these studies recognizes a 58 kDa protein on western blot which could correspond either to a shorter splice variant of Krit1 or to another protein. To address this question, we studied by sedimentation on sucrose cushion the binding of purified His-tagged full-length Krit1 to in vitro polymerized microtubules (MT). When 40 pmoles of full-length Krit1 were incubated with MT polymerized from 200 pmoles of purified tubulin, 60% of the protein co-sedimented with MT (Fig. 6A), demonstrating a direct interaction of Krit1 with MT. Remarkably, the contaminant proteins contained in Krit1 preparations, even those present at the same concentration as Krit1, did not co-sediment with MT (Fig. 6A), highlighting the specificity of Krit1 interaction with MT. To map the domain responsible for this interaction, we studied the binding of different fragments of Krit1 in the same conditions. Krit1-NTer fragment bound strongly to MT (45%). Krit1 bears a basic stretch of six lysines and arginine on its N-terminus which could interact with MT. Mutations of amino acids 47KKRK50 in four alanines almost completely abolished Krit1 binding to MT (Fig. 6A) whereas this mutant was still able to interact with ICAP-1 (data not shown). GST-HypoKrit1 also interacted with MT. However, by contrast to full-length Krit1 and Krit1-NTer, only 20% of GST-HypoKrit1 bound to MT (Fig. 6A). In control, GST alone did not bind to MT (Fig. 6B). The truncation in the F3 sub-domain of GST-HypoKrit1 almost completely abolished the co-sedimentation of GST-hypoKrit1 Δ C with MT (Fig. 6A). Thus two sites are responsible for the interaction of Krit1 with microtubules: a basic stretch of residues located in the N-terminal part of the protein centered on residues 46 to 50 with high affinity for MT and a second site located on the F3 sub-domain with low affinity for MT.

Rap 1 and ICAP-1 inhibit in vitro Krit1 binding to microtubules.

Having shown that MT bind to the N- and C- termini of Krit1, we asked whether ICAP-1 or Rap1, which bind respectively to Krit1 N- and C-termini, could modulate Krit1 interaction with MT. Thus, we measured the binding of 40 pmoles of Krit1 to MT in presence of 200 pmoles of Rap1GTP γ S or GST-ICAP-1. Rap1GTP γ S alone was not recruited to MT and less than 10% of GST-ICAP-1 bound to MT (Fig. 6B). Remarkably, both Rap1GTP γ S and GST-ICAP-1 inhibited Krit1 binding to MT whereas GST alone had no effect (Fig. 6B). Similar inhibition was obtained using Rap1B isoform (data not shown). However, ICAP-1 was a more potent inhibitor than Rap1GTP γ S at these concentrations (80 % inhibition versus 50%). It is unlikely that ICAP-1 effect would be due to a competition with Krit1 for binding to MT since only 20 pmoles of GST-ICAP-1 bound to the 150 pmoles of tubulin, polymerized in MT, leaving around 130 pmoles of tubulin available for interaction with Krit1.

YFP-Krit1 co-localizes with CFP-labelled microtubules in transfected BHK cells and is delocalized from microtubules by activated Rap1.

To confirm our in vitro results in a cellular context, we co-expressed Krit1 fused to YFP together with CFP-tubulin in BHK cells. While YFP-ARNO signal, used as a negative control, was diffuse in the cytosol, YFP-Krit1 signal was superimposable to the CFP-labelled microtubules signal indicating that YFP-Krit1 was localized along microtubules from MTOC to periphery. Co-expression of activated mutant of Rap1, HA-Rap1V12, flattened the cells which became spread and displayed numerous membrane spikes, a phenotype also observed with HA-Rap1V12 alone (data not shown). Remarkably, YFP-Krit1 was no longer co-localized with CFP-labelled microtubules in Rap1V12 expressing BHK cells. Thus, these experiments support our in vitro observations that Krit1 binds to microtubules and that this binding is inhibited by Rap1GTP .

Rap1 enhances HypoKrit1 binding to asolectin vesicles.

An other feature of Krit1 is its capacity to bind to phospholipids. We wondered whether Rap1, which binds to Krit1 FERM domain, could modulate Krit1 association with membranes. Remarkably, when 3 μ M of Rap1GTP γ S were added to 0.5 μ M GST-HypoKrit1, we observed a stimulation of GST-HypoKrit1 binding to asolectin vesicles, (Fig. 8A). A fraction of Rap1GTP γ S also sedimented with the vesicles. Since the recombinant unmodified Rap1 that we used did not bind to lipids by itself (Fig.8A), this fraction actually corresponds to Rap1

complexed with HypoKrit1 (Fig. 8A). Moreover, the stimulation of GST-HypoKrit1 binding to asolectin vesicles by Rap1GTP γ S was dose-dependent, up to 6-fold (Fig. 8B).

DISCUSSION

In this paper, we confirm that Krit1 specifically interacts in vitro with Rap1 and preferentially with active Rap1 (GTP-bound form), the criteria for Krit1 being a “bona-fide” effector of Rap1. We show for the first time that Krit1 exists in a closed conformation in which its N-terminus interacts with its C-terminus. ICAP-1 binding to the N-terminal NPAY motif disrupts this interaction, whereas Rap1 binding to the C-terminal FERM domain does not. Moreover, we show that Krit1, Rap1 and ICAP-1 can form a ternary complex in vitro.

Krit1 binds in vitro to microtubules via two sites on its N and C-termini. Remarkably, Rap1 and ICAP-1 inhibit in vitro Krit1 binding to microtubules. In transfected BHK cells, YFP-Krit1 localizes along CFP-labelled microtubules and is delocalized from microtubules by co-expression of activated Rap1V12. Finally we show that Krit1 binds to phospholipids on membranes and that Rap1 enhances this binding.

Krit1 is an effector of Rap1

Our detailed biochemical study demonstrates that Krit1 interacts specifically with Rap1 ending the debate about this question. Indeed, both N-truncated Krit1, which we called HypoKrit1, (corresponding to the yeast two-hybrid Rap1 partner originally identified) and the full-length protein interact with Rap1, as shown by pull-down and asolectin vesicle sedimentation experiments. Moreover, HypoKrit1 interacts with a higher affinity with Rap1GTP γ S than with Rap1GDP, indicating that Krit1 is a downstream effector of Rap1. Similar results were obtained with FLAG-tagged full-length Krit1 (data not shown). Our results differ substantially from those of Zhang et al who failed to observe an interaction between the two proteins [11]. This discrepancy might be related to the methods applied. These authors used in vitro translation of Rap1 and Krit1. The amount of proteins produced might not be sufficient for co-immunoprecipitation, since micromolar concentrations of the two proteins were necessary in our hands to observe a complex. Consistently, an interaction of low affinity ($K_d=4.7 \mu\text{M}$) was found between Krit1 and Rap1B, a very close homolog of Rap 1A [29]. We did not detect any

interaction of H-Ras with Krit1 as previously reported [10], [30], [29]. Thus, it appears that Krit1 is a specific effector of Rap1, suggesting that it is involved in a Ras-independent, Rap1-dependent pathway. Even though it has been proposed that Rap1 may bind to Krit1 F1 sub-domain because this sub-domain bears homology with a computerized model of Ras Binding Domain (RBD) [31], the absence of interaction between HypoKrit1 Δ C and Rap1 rather suggests that Rap1 interacts with the PTB-like F3 sub-domain. Similarly, talin and radixin FERM domains interact via their F3 sub-domain with respectively integrin and ICAM-2 cytoplasmic tails, as shown by co-crystal structures [32],[33]. Further mutagenesis studies will be necessary to map precisely the site for Rap1 interaction on Krit1 FERM domain.

Krit1, like other FERM proteins, adopts closed and opened conformations and binds to PIP₂

The molecular modeling of the last 300 amino acid residues of Krit1 that we generated corroborates the existence of a FERM domain at the C-terminus of the protein. FERM domains are involved in localizing proteins to the plasma membrane. It has been shown by sedimentation experiments and crystallographic studies that they bind to PIP₂ (for instance radixin [30], talin [34]) via the interaction of the polar head of the lipid with a basic cleft present between F1 and F3 sub-domains. Consistently, we show that Krit1 binds to PIP₂. Interestingly, several basic residues are exposed to the F1-F3 cleft on the Krit1 FERM model that we generated. Mutagenesis analyses of these residues will help to determine whether the binding site of the polar head of PIP₂ on Krit1 is similar to that of radixin.

Many members of the FERM family undergo intra- and/or inter- molecular folding of their C-terminus onto their N-terminal FERM domain [21]. Consistently, we demonstrate the interaction of the N-terminus of Krit1 with its C-terminus, both parts being produced separately. Cis or trans interaction between these two domains are equally possible and would lead to either an intramolecular folding in a closed conformation or an intermolecular folding in an anti-parallel homodimer like talin. Furthermore, we have shown that the N-terminal NPAY motif is involved in the interaction, which suggests that the PTB-like F3 sub-domain of the FERM is the C-terminal counterpart. As such, in the dormant form of moesin, F3 sub-domain is masked by the N-terminal extended actin binding tail domain [27]. Moreover, we show that ICAP-1 binding disrupts Krit1 N and C-termini interaction. This interaction, as well as its disruption by ICAP-1, could be verified on the full-length protein by fluorescence resonance energy transfer (FRET) of

Krit1 fused to YFP and CFP at its extremities. This could represent a crucial mechanism of regulation of Krit1 activity. Indeed, both NPAY motif and PTB-like F3 sub-domain are binding sites for other partners, such as ICAP-1, phospholipids and yet unknown partners most likely trans-membrane or peri-membrane proteins. Masking of these two sites may prevent Krit1 to interact with other proteins until it is delivered to its target (s). It has been shown that Krit1 interacts with the CCM2 gene product malcavernin, a PTB domain protein, in the context of a Rac/MEKK3/MKK3 signalling complex which activates p38 MAPK kinase [35]. Krit1-CCM2 interaction does not involve the NPAY motif and a ternary complex can form between Krit1, CCM2 and ICAP-1. It is possible that Krit1, through its interaction with different partners on the plasma membrane, participates in several but linked signalling pathways involved in angiogenesis [35].

Rap1 and ICAP-1 regulate Krit1 localization to microtubules and membranes

Among the FERM family members, ERM proteins and talin provide a regulated linkage between membrane proteins and the cortical actin cytoskeleton. No actin-binding site has been reported on Krit1. Consistently, purified Krit1 does not interact with in vitro polymerized actin (Eric Macia, personal communication) nor does YFP-Krit1 localize in cells to phalloidin-labelled F-actin (data not shown). Instead, we confirm the previous report that Krit1 is a microtubule-associated protein [22] by showing that it co-localizes with microtubules in cells and that it interacts directly with in vitro polymerized microtubules. Moreover, our results show that Krit1 binds to MT through two sites: one basic site in the N-terminal part of the protein located on residues 46 to 51 with high affinity for MT and a second on the C-terminus in the F3 sub-domain with low affinity for MT. The N-terminal basic motif has also been described as a functional nuclear localization sequence [39], suggesting that it could be involved in the shuttling of Krit1 between the microtubules and the nucleus. Remarkably, the contribution of these two sites to the binding to MT is additive (Fig. 6A). Since we show that the N-terminus of Krit1 interacts with the C-terminus, it is most likely that these two MT binding sites actually form a continuous surface on the closed protein. We show that ICAP-1 and Rap1 both inhibit the binding of Krit1 to MT. Two hypotheses can be proposed concerning the mechanism of this inhibition. The first one is that they directly mask the surface that binds to MT. Indeed our results show that MT and Rap1 both bind to the last fifty residues of Krit1. It is not so clear for the basic stretch which lies

between residues 46 to 51. ICAP-1 binds further on the primary sequence on the $_{191}\text{NPAY}_{194}$ motif. It is possible however that these two sites are actually close in the folded protein. The second hypothesis is that ICAP-1 binding provokes structural changes of the basic site that lead to a decrease of its affinity for MT. Nevertheless, the fact that ICAP-1 is a more potent inhibitor than Rap1 correlates well with, for one part, its stronger binding to Krit1 at the micromolar concentrations used in these experiments and, for the second part, with the higher contribution to the binding to MT of the basic stretch than the C-terminal site.

At the cell periphery, Rap1 shuttles between recycling endosomes and the plasma membrane, its GTP form being localized at the plasma membrane [36]. Interestingly, we show that Rap1GTP γ S stimulates HypoKrit1 binding to artificial membranes. HypoKrit1 is not recruited to membranes through Rap1 because the unmodified Rap1 that we used does not bind to membranes. Instead, Rap1 binding to Krit1 FERM domain most likely induces a conformational change of the PIP2 binding pocket that gives HypoKrit1 a better affinity for PIP2. Our attempts to observe Rap1 stimulation of full-length Krit1 binding to asolectin vesicles were not successful even in the presence of ICAP-1, whose binding should unmask Krit1 FERM domain (data not shown). Several experimental caveats may be responsible for this negative result. In absence of its C-terminal lipid anchor, Rap1 positioning toward Krit1 and the membrane may not be optimized and therefore the complex not fully stabilized. Moreover ICAP-1 may not be sufficient to stabilize Krit1 in its opened conformation. Interaction with another partner may be required for the protein to be stably opened.

Krit1 localization on microtubules and its delocalization by activated Rap1 is very similar to reported results on RAPL, another Rap1 effector. Indeed, RAPL also localizes on MT in endothelial cells and directly binds to in vitro polymerized MT [37]. In wound healing assays, RAPL localizes on MT oriented toward the leading edge, an area where Rap1 is highly activated and its interaction with Rap1 is required for directional migration [37]. Moreover, co-expression of Rap1V12 also induces dissociation of RAPL from MT [37]. In lymphocytes, RAPL moves dynamically from the peri-nuclear region to the leading edge upon chemokine stimulation and activated Rap1 triggers the association of RAPL with $\alpha\text{L}\beta\text{2}$ leading to the redistribution of this integrin to the immunological synapse [4]. In addition to integrin activation, Rap1 induces cell polarization and facilitates cell migration. Expression of activated Rap1 polarizes lymphocytes, generating a leading edge at the front and a uropod at the back. It also stimulates lymphocyte

endothelium transmigration [38] and directional migration of endothelial cells [37]. Therefore, delivery of Rap1 effectors to focal adhesions by the MT network might participate in the polarized activation of integrins. In line, targeting of MT in close vicinity of adhesion foci on the plasma membrane has been reported [39], as well as regulation of the turn-over of focal adhesions by MT [23], [24]. Based on our results, we propose a model of regulation of Krit1 binding to MT and plasma membrane; in the cell, Krit1 would be transported in its closed conformation along MT toward the plasma membrane. When reaching the membrane, Krit1 would detach from MT and be captured by activated Rap1 and ICAP-1 on the plasma membrane (Fig. 9). In the absence of ICAP-1, Rap1GTP would bind to Krit1 favouring its detachment from the MT and its binding to the plasma membrane without, however, opening it. This complex could serve as a stock for a rapid delivery of Krit1 to its target sites on the plasma membrane.

An important breakthrough in unraveling the Rap1-dependent pathway in integrin activation has been achieved recently by Han et al [13]. Their work demonstrates that Rap1 promotes talin binding to the cytoplasmic tail of $\beta 3$ and $\beta 1$ integrins. They show that Rap1 induces the formation of an integrin activation complex which contains talin and RIAM, a Rap1 effector. RIAM is known to bind to profilin and Ena/VASP [5] suggesting that it could participate in actin network formation at the level of focal adhesion [13].

Concerning activation of $\beta 1$ integrin per se, i. e. its switch to high affinity conformation, our present data and Han's lead us to hypothesize that this Rap1-dependent activation complex could contain Krit1. Its binding to ICAP-1 would displace ICAP-1 from its inhibitory site on $\beta 1$ integrin, therefore allowing talin binding and subsequent $\beta 1$ conformational changes. Further work is in progress to determine whether Krit1 is targeted by the microtubule network to focal adhesions and whether Rap1, RIAM and ICAP-1 regulate this localization. Furthermore, functional studies will investigate the role of Krit1 on cell adhesion to determine whether Krit1 is involved in the Rap1-dependent integrin activation pathway.

MATERIAL AND METHODS

Plasmid constructions - pcDNA4/V5-HISA-FLAG-Krit1 and pCDNA4/V5-HISA-FLAG-ICAP-1 were kindly provided by D.A. Marchuk (Duke University Medical Center, Durham, NC). Krit1 was sub-cloned in pET21d (Novagen, Fontenay-sous-Bois, France) and pEYFP-N1 (Clontech,

Saint-Germain-en-Laye, France), HypoKrit1 (208 to 736) in pGEX-2T (Roche Diagnostics, Meylan, France). Krit1-Nter (1-207) was sub-cloned in pQE 30 (Qiagen) and pETGEX-CT (National Institute of Genetics, Japan). Asn192Ala-Tyr195Ala substitutions, alanine substitutions of ⁴⁷KRKK⁵⁰ and introduction of a stop codon at aa 686 were produced using the QuikChange mutagenesis kit (Stratagene, Amsterdam, The Netherlands). pMT2-HA-Rap1A and pMT2-HA-Rap1AV12 were kindly provided by J. L. Bos (University Medical Center, Utrecht, The Netherlands). C-terminal-deleted (1-167) Rap1A was sub-cloned into pET16b (Novagen). ICAP-1 was sub-cloned in pGEX-2T.

Purification of recombinant proteins - The expression of Krit1 and Krit1 KRKK/AAAA in *Escherichia. coli* BL21(DE3)codon+ cells (Stratagene) was induced at an optical density (OD₆₀₀) of 0.8 with 0.2 mM isopropyl-β-D thio-galactopyranoside and grown for an additional 16 h at 18°C. His-tagged Rap1, His-tagged Krit1-Nter WT and APAA, GST-HypoKrit1, GST-HypoKrit1ΔC, Krit1-Nter-GST, and GST-ICAP-1 were produced in *Escherichia. coli* BL21 gold (Stratagene) induced with 0.2 mM IPTG at OD 0.8 for 3 h at 28°C. Purifications were performed according to manufacturer instructions using the nickel-charged resin Ni-NTA (Qiagen, Courtaboeuf, France) for His-Tagged proteins or Glutathione sepharose 4B (GE Healthcare Europe GmbH, Orsay, France) for GST fusions. Purified His-tagged Krit1 WT and KRKK/AAAA were dialyzed and concentrated against 50 mM phosphate buffer pH 8.0, 120 mM NaCl, 10 % glycerol, DTT 1 mM. All other proteins were dialyzed and concentrated in 20 mM Tris-HCl pH 7.5, 120 mM NaCl, 1 mM MgCl₂, and 10% glycerol and supplemented with 20 μM GDP for His-tagged Rap1. A fraction of purified GST-ICAP-1 was cleaved by thrombin according to manufacturer instructions (GE Healthcare). Protein concentration was determined by SDS-PAGE and fluorometric analysis of Sypro Orange (Amresco, Interchim, Montluçon, France) stained gel using a Fuji LAS3000 fluorescence imaging system.

Preloading of Rap1 with GDP or GTPγS - Purified Rap1 was incubated for 45 min at 30°C in 50 mM Tris-HCl pH 7.5, 120 mM NaCl, 1 mM MgCl₂, 2 mM EDTA, 10% glycerol and 2 mM GTPγS or GDP (Roche Diagnostics). The loaded nucleotide was stabilized in the nucleotide site by addition of 5 mM MgCl₂.

GST pull-down - Purified GST-fusions bound to 20 μl of glutathione beads (GE Healthcare) were incubated under agitation with purified His-tagged proteins as indicated for 2 h at 4°C in PD buffer (50 mM Tris-HCl pH 7.5, 120 mM NaCl, 1 mM MgCl₂, 10% glycerol, 1% NP-40, 2 mM

DTT, protease inhibitors) in a final volume of 50 μ l. Beads were washed three times in 1 ml of PD buffer and eluted with 30 μ l of Laemmli sample buffer. Input and bound proteins were analyzed by Sypro Orange (Amresco) staining of the gel or by western blotting.

Cell culture and transfection: Baby Hamster Kidney (BHK) cells were grown in BHK-21 medium (Invitrogen BV, Leek, The Netherlands) containing 5% fetal calf serum, 10% tryptose phosphate broth, 100 units/ml penicillin, 100 μ g/ml streptomycin and 2 mM L-Glutamine. The cells were transfected with Fugene6 transfection reagent (Roche Diagnostics) according to the manufacturer's instructions.

FLAG pull-down: BHK cells were transfected with pcDNA4/V5-HISA-FLAG-Krit1. Forty eight hours after transfection, cells were washed with PBS and scrapped in PD buffer. After a 15 min incubation at 4°C, cells were centrifuged at 14 000g for 30 min at 4°C. The supernatant was incubated with mouse anti-FLAG M2 coupled to agarose beads (Sigma Aldrich L'Isle d'Abeau Chesnes, France) for 2 hours at 4°C. FLAG-Krit1 trapped on beads was incubated with 3 μ M of Rap1GTP γ S, 7 μ M of ICAP-1 or both for 2 hours at 4°C under agitation. Beads were then washed three times with PD buffer and bound proteins were eluted with 200 μ g/ml of FLAG peptide in PD buffer. Input and eluted proteins were analyzed by SDS-PAGE and Sypro Orange staining of the gel.

Microtubule sedimentation experiments:

-Tubulin purification and polymer preparation: Purified lamb brain tubulin was polymerized for 15 min at 37°C in BRB50 buffer (50 mM PIPES pH 6.8, 1mM EGTA, 1 mM MgCl₂) containing 1 mM GTP, 5 mM MgCl₂ and 10 % glycerol [40]. Then, every 10 min, 8, 80, and 800 μ M taxol were added at 37°C. The mixture was layered onto 28 μ l of 50% glycerol in BRB50 buffer containing 1 mM GTP and 80 μ M taxol and centrifuged at 16000 g for 10 min at 25°C. The pellet was re-suspended in the same buffer.

-Sedimentation experiments: Polymerized microtubules corresponding to approximately 150 pmoles of tubulin were incubated with the indicated proteins in BRB50 buffer pH 7.5, in 20 μ l for 30 min at 25°C. The reaction mixture was layered onto 20 μ l of 30% glycerol in BRB50 buffer pH 7.5 and centrifuged at 16 000 g for 10 min at 25°C. The pellets were resuspended in 40 μ l of 15 % glycerol in BRB50 buffer pH 7.5. The percentage of proteins cosedimented with microtubules was determined by SDS-PAGE and fluorometric analysis of the Sypro Orange stained gel using fluorescence imaging or by western blotting.

Immunofluorescence and cell microscopy:

BHK cells were co-transfected with pEYFP-Krit1 and pECFP-tubulin with or without pMT2-HA-Rap1V12. Twenty-four hours after transfection, cells were fixed in 4% PFA for 20 minutes and processed for immunofluorescence analysis as already described [41]. HA-Rap1V12 was labelled with 3F10 anti-HA monoclonal antibody (Roche Diagnostics). Confocal microscopy analysis was carried out using a Leica TCS-SP5 microscope (Leica Microsystems SAS, Rueil-Malmaison, France).

Asolectin vesicles and liposome sedimentation experiments:

- *Asolectin vesicles and liposomes preparation:* Asolectin (Sigma Aldrich) vesicles were prepared by the reverse phase method [42] and sucrose-loaded liposomes (plasma membrane mix: 40% PC, 15% PE, 20% cholesterol, 25% PS, 0.2 % NBD-PE; 2 mM lipids) were prepared by the extrusion method [43]. Lipids in chloroform were purchased from Avanti Polar Lipids except for egg PC (Sigma Aldrich) and NBD-PE (Molecular Probes Europe, Leiden, The Netherlands)

- *Sedimentation experiments:* Proteins were incubated for 20 min at 25 °C with sucrose-loaded liposomes or asolectin vesicles in 20 mM Tris-HCl pH 8.0, 120 mM NaCl, 1mM MgCl₂, 10 % glycerol, 1 mM DTT and were centrifuged for 20 min at 400000g at 20 °C. The percentage of proteins in the supernatant and pellet was determined by fluorometric analysis of the Sypro-Orange stained gel using fluorescence imaging.

Modelling of Krit1 FERM domain - The Psi-Blast [44] web tools were used to obtain alignments of Krit1 last 300 residues with different template sequences. The structure of radixin (pdb entry; 1GC6) was used as template for F1 FERM domain and that of talin (pdb entry: 1Y19) for F2 and F3 FERM domains. The alignments were improved manually, taking into account the predicted secondary structure of Krit1 and the secondary structures of talin and radixin. One hundred models of F1, F2 and F3 domains were constructed separately by comparative modelling with the MODELLER 7 program [45]. The best model was retained for each FERM domain and the side chains were repositioned in optimized conformations, using SCWRL[46] and SCit web server [47]. The models were finally subjected to energy minimization. The stability of these models was assayed by molecular dynamics simulations using the Gromos 96 force field implemented in GROMACS version 3.2.1 [48]. Since there is a good conservation of the spatial arrangement of F1-F2-F3 among the cristallized FERM domains, the three modeled Krit1

subdomains were manually positioned according to the arrangement of radixin FERM domain. Structures were visualized with Pymol (Delano Scientific LLC, USA)

ACKNOWLEDGEMENTS

We are thankful to Frédéric Brau for excellent technical support in confocal microscopy. We thank Daniel Bouvard, Julie Milanini, Michel Franco and Eric Macia for useful discussions and critical reading. We thank D.A. Marchuk for providing us with Krit1 and ICAP-1 cDNAs, and J. L. Bos for Rap1 cDNA. We thank Alfred Wittinghofer for providing H-Ras. This work has been supported by the Association pour la Recherche sur le Cancer.

REFERENCES

1. Bos, J. L. (2005) Linking Rap to cell adhesion, *Curr Opin Cell Biol.* 17, 123-8.
2. Caron, E. (2003) Cellular functions of the Rap1 GTP-binding protein: a pattern emerges, *J Cell Sci.* 116, 435-440.
3. Kooistra, M. R., Dube, N. & Bos, J. L. (2007) Rap1: a key regulator in cell-cell junction formation, *J Cell Sci.* 120, 17-22.
4. Katagiri, K., Maeda, A., Shimonaka, M. & Kinashi, T. (2003) RAPL, a Rap1-binding molecule that mediates Rap1-induced adhesion through spatial regulation of LFA-1, *Nat Immunol.* 6, 6.
5. Lafuente, E. M., van Puijenbroek, A. A., Krause, M., Carman, C. V., Freeman, G. J., Berezovskaya, A., Constantine, E., Springer, T. A., Gertler, F. B. & Boussiotis, V. A. (2004) RIAM, an Ena/VASP and Profilin ligand, interacts with Rap1-GTP and mediates Rap1-induced adhesion, *Dev Cell.* 7, 585-95.
6. Arthur, W. T., Quilliam, L. A. & Cooper, J. A. (2004) Rap1 promotes cell spreading by localizing Rac guanine nucleotide exchange factors, *J Cell Biol.* 167, 111-22.
7. Krugmann, S., Andrews, S., Stephens, L. & Hawkins, P. T. (2006) ARAP3 is essential for formation of lamellipodia after growth factor stimulation, *J Cell Sci.* 119, 425-32.
8. Jeon, T. J., Lee, D. J., Merlot, S., Weeks, G. & Firtel, R. A. (2007) Rap1 controls cell adhesion and cell motility through the regulation of myosin II, *J Cell Biol.* 176, 1021-33.
9. Zhang, Z., Rehmann, H., Price, L. S., Riedl, J. & Bos, J. L. (2005) AF6 negatively regulates Rap1-induced cell adhesion, *J Biol Chem.* 280, 33200-5.
10. Serebriiskii, I., Estojak, J., Sonoda, G., Testa, J. R. & Golemis, E. A. (1997) Association of Krev-1/rap1a with Krit1, a novel ankyrin repeat-containing protein encoded by a gene mapping to 7q21-22, *Oncogene.* 15, 1043-9.
11. Zhang, J., Clatterbuck, R. E., Rigamonti, D., Chang, D. D. & Dietz, H. C. (2001) Interaction between krit1 and icap1alpha infers perturbation of integrin beta1-mediated angiogenesis in the pathogenesis of cerebral cavernous malformation, *Hum Mol Genet.* 10, 2953-60.

12. Revencu, N. & Vikkula, M. (2006) Cerebral cavernous malformation: new molecular and clinical insights, *J Med Genet.* *43*, 716-21.
13. Han, J., Lim, C. J., Watanabe, N., Soriani, A., Ratnikov, B., Calderwood, D. A., Puzon-McLaughlin, W., Lafuente, E. M., Boussiotis, V. A., Shattil, S. J. & Ginsberg, M. H. (2006) Reconstructing and deconstructing agonist-induced activation of integrin alphaIIb beta3, *Curr Biol.* *16*, 1796-806.
14. Calderwood, D. A. (2004) Integrin activation, *J Cell Sci.* *117*, 657-66.
15. Bouvard, D., Vignoud, L., Dupe-Manet, S., Abed, N., Fournier, H.-N., Vincent-Monegat, C., Retta, S. F., Fassler, R. & Block, M. R. (2003) Disruption of Focal Adhesions by Integrin Cytoplasmic Domain-associated Protein-1alpha, *J. Biol. Chem.* *278*, 6567-6574.
16. Bouvard, D., Aszodi, A., Kostka, G., Block, M. R., Albiges-Rizo, C. & Fassler, R. (2007) Defective osteoblast function in ICAP-1-deficient mice, *Development.* *134*, 2615-25.
17. Bouvard, D., Millon-Fremillon, A., Dupe-Manet, S., Block, M. R. & Albiges-Rizo, C. (2006) Unraveling ICAP-1 function: toward a new direction?, *Eur J Cell Biol.* *85*, 275-82.
18. Zawistowski JS, S. I., Lee MF, Golemis EA, Marchuk DA. (2002) KRIT1 association with the integrin-binding protein ICAP-1: a new direction in the elucidation of cerebral cavernous malformations (CCM1) pathogenesis, *Hum Mol Genet.* *11*, 389-96.
19. Marchuk, D. A., Srinivasan, S., Squire, T. L. & Zawistowski, J. S. (2003) Vascular morphogenesis: tales of two syndromes, *Hum Mol Genet.* *12 Spec No 1*, R97-112.
20. Clatterbuck, R. E., Eberhart, C. G., Crain, B. J. & Rigamonti, D. (2001) Ultrastructural and immunocytochemical evidence that an incompetent blood-brain barrier is related to the pathophysiology of cavernous malformations, *J Neurol Neurosurg Psychiatry.* *71*, 188-92.
21. Bretscher, A., Edwards, K. & Fehon, R. G. (2002) ERM proteins and merlin: integrators at the cell cortex, *Nat Rev Mol Cell Biol.* *3*, 586-99.
22. Gunel, M., Laurans, M. S. H., Shin, D., DiLuna, M. L., Voorhees, J., Choate, K., Nelson-Williams, C. & Lifton, R. P. (2002) KRIT1, a gene mutated in cerebral cavernous malformation, encodes a microtubule-associated protein, *PNAS.* *99*, 10677-10682.
23. Kaverina, I., Rottner, K. & Small, J. V. (1998) Targeting, capture, and stabilization of microtubules at early focal adhesions, *J Cell Biol.* *142*, 181-90.
24. Small, J. V. & Kaverina, I. (2003) Microtubules meet substrate adhesions to arrange cell polarity, *Current Opinion in Cell Biology.* *15*, 40-47.
25. Smith, W. J. & Cerione, R. A. (2002) Crystallization and preliminary crystallographic analysis of the ezrin FERM domain, *Acta Crystallogr D Biol Crystallogr.* *58*, 1359-61.
26. Hamada, K., Shimizu, T., Matsui, T., Tsukita, S. & Hakoshima, T. (2000) Structural basis of the membrane-targeting and unmasking mechanisms of the radixin FERM domain, *Embo J.* *19*, 4449-62.
27. Pearson, M. A., Reczek, D., Bretscher, A. & Karplus, P. A. (2000) Structure of the ERM protein moesin reveals the FERM domain fold masked by an extended actin binding tail domain, *Cell.* *101*, 259-70.
28. Balla, T. (2005) Inositol-lipid binding motifs: signal integrators through protein-lipid and protein-protein interactions, *J Cell Sci.* *118*, 2093-104.
29. Wohlgemuth, S., Kiel, C., Kramer, A., Serrano, L., Wittinghofer, F. & Herrmann, C. (2005) Recognizing and defining true Ras binding domains I: biochemical analysis, *J Mol Biol.* *348*, 741-58.
30. Serebriiskii, I., Khazak, V. & Golemis, E. A. (1999) A two-hybrid dual bait system to discriminate specificity of protein interactions, *J Biol Chem.* *274*, 17080-7.

31. Kiel, C., Wohlgemuth, S., Rousseau, F., Schymkowitz, J., Ferkinghoff-Borg, J., Wittinghofer, F. & Serrano, L. (2005) Recognizing and defining true Ras binding domains II: in silico prediction based on homology modelling and energy calculations, *J Mol Biol.* 348, 759-75.
32. Garcia-Alvarez, B., de Pereda, J. M., Calderwood, D. A., Ulmer, T. S., Critchley, D., Campbell, I. D., Ginsberg, M. H. & Liddington, R. C. (2003) Structural determinants of integrin recognition by talin, *Mol Cell.* 11, 49-58.
33. Hamada, K., Shimizu, T., Yonemura, S., Tsukita, S., Tsukita, S. & Hakoshima, T. (2003) Structural basis of adhesion-molecule recognition by ERM proteins revealed by the crystal structure of the radixin-ICAM-2 complex, *EMBO J.* 22, 502-514.
34. Martel, V., Racaud-Sultan, C., Dupe, S., Marie, C., Paulhe, F., Galmiche, A., Block, M. R. & Albiges-Rizo, C. (2001) Conformation, localization, and integrin binding of talin depend on its interaction with phosphoinositides, *J Biol Chem.* 276, 21217-27.
35. Zawistowski, J. S., Stalheim, L., Uhlik, M. T., Abell, A. N., Ancrile, B. B., Johnson, G. L. & Marchuk, D. A. (2005) CCM1 and CCM2 protein interactions in cell signaling: implications for cerebral cavernous malformations pathogenesis, *Hum Mol Genet.* 14, 2521-31.
36. Bivona, T. G., Wiener, H. H., Ahearn, I. M., Silletti, J., Chiu, V. K. & Philips, M. R. (2004) Rap1 up-regulation and activation on plasma membrane regulates T cell adhesion, *J Cell Biol.* 164, 461-70.
37. Fujita, H., Fukuhara, S., Sakurai, A., Yamagishi, A., Kamioka, Y., Nakaoka, Y., Masuda, M. & Mochizuki, N. (2005) Local activation of Rap1 contributes to directional vascular endothelial cell migration accompanied by extension of microtubules on which RAPL, a Rap1-associating molecule, localizes, *J Biol Chem.* 280, 5022-31.
38. Shimonaka, M., Katagiri, K., Nakayama, T., Fujita, N., Tsuruo, T., Yoshie, O. & Kinashi, T. (2003) Rap1 translates chemokine signals to integrin activation, cell polarization, and motility across vascular endothelium under flow, *J. Cell Biol.* 161, 417-427.
39. Krylyshkina, O., Anderson, K. I., Kaverina, I., Upmann, I., Manstein, D. J., Small, J. V. & Toomre, D. K. (2003) Nanometer targeting of microtubules to focal adhesions, *J Cell Biol.* 161, 853-9.
40. Lee, Y. C., Samson, F. E., Jr., Houston, L. L. & Himes, R. H. (1974) The in vitro polymerization of tubulin from beef brain, *J Neurobiol.* 5, 317-30.
41. Franco, M., Boretto, J., Robineau, S., Monier, S., Goud, B., Chardin, P. & Chavrier, P. (1998) ARNO3, a Sec7-domain guanine nucleotide exchange factor for ADP ribosylation factor 1, is involved in the control of Golgi structure and function, *Proc Natl Acad Sci U S A.* 95, 9926-31.
42. Franco, M., Chardin, P., Chabre, M. & Paris, S. (1995) Myristoylation of ADP-ribosylation factor 1 facilitates nucleotide exchange at physiological Mg²⁺ levels, *J Biol Chem.* 270, 1337-41.
43. Mayer, L. D., Hope, M. J. & Cullis, P. R. (1986) Vesicles of variable sizes produced by a rapid extrusion procedure, *Biochim Biophys Acta.* 858, 161-8.
44. Altschul, S. F., Madden, T. L., Schaffer, A. A., Zhang, J., Zhang, Z., Miller, W. & Lipman, D. J. (1997) Gapped BLAST and PSI-BLAST: a new generation of protein database search programs, *Nucleic Acids Res.* 25, 3389-402.
45. Marti-Renom, M. A., Stuart, A. C., Fiser, A., Sanchez, R., Melo, F. & Sali, A. (2000) Comparative protein structure modeling of genes and genomes, *Annu Rev Biophys Biomol Struct.* 29, 291-325.

46. Canutescu, A. A., Shelenkov, A. A. & Dunbrack, R. L., Jr. (2003) A graph-theory algorithm for rapid protein side-chain prediction, *Protein Sci.* 12, 2001-14.
47. Gautier, R., Camproux, A. C. & Tuffery, P. (2004) SCit: web tools for protein side chain conformation analysis, *Nucleic Acids Res.* 32, W508-11.
48. Van Der Spoel, D., Lindahl, E., Hess, B., Groenhof, G., Mark, A. E. & Berendsen, H. J. (2005) GROMACS: fast, flexible, and free, *J Comput Chem.* 26, 1701-18.

FIGURE LEGENDS

Fig. 1. Krit1 contains a putative FERM domain and binds to PIP₂.

(A) Radixin-IP3 co-crystal structure. IP3 is in yellow, basic residues of F1 (K53, K60, K63, K64) and F3 (R273, R275, R279) domains are in red. The Tryptophan W58 is in green. (B) Homology models of F1, F2 and F3 domains of Krit1. The three independently modeled sub-domains have been manually arranged as on radixin structure. Basic residues of F1 (K475, K479, R485) and F3 (K713, K720, K724) domains are in red. The Tryptophan W487 is in green. (C) Krit1 (1 μM) was incubated with plasma membrane mix liposomes (0.75 mM) containing or not 2 % PIP₂ at various NaCl concentrations. After centrifugation, proteins present in the supernatant (S) and the pellet (P) were analyzed by SDS-PAGE and quantified by fluorometry. Protein precipitation in the absence of liposomes has been subtracted. Bands below Krit1 band are E.Coli contaminants that also bind to PIP₂.

Fig.2. Krit1 N and C terminal parts associate together via the NPAY motif and ICAP-1 disrupts this association.

(A) Schematic representation of Krit1 fragments used. FERM domain : Four-point one, Ezrin, Radixin, Moesin; PTB-like: Phosphotyrosine-binding domain. ANK: Ankyrin repeats. (B) GST-pull-down of 100 nM Krit1-Nter WT or mutant on 100 nM GST-HypoKrit1 or GST alone following the experimental procedure detailed in material and methods. (C). GST-pull-down of 5 μM Krit1-Nter on 3.5 μM GST-HypoKrit1 in presence of 5 μM ICAP-1. In (A) GST-fusions were immunoblotted with GST antibodies. In (B) and (C), GST-fusions were stained with Ponceau Red. Krit1-Nter and ICAP-1 were immunoblotted with His-tag and ICAP-1 antibodies

respectively. Inputs correspond to 1/20 of total proteins. These results are representative of three independent experiments.

Fig. 3. Rap1 binds to Krit1 C-terminus preferentially in its Rap1GTP form.

(A) GST-pull down of 1 μ M Rap1GDP, Rap1GTP γ S or H-RasGTP γ S on 10 μ M GST-HypoKrit1 or GST alone. Inputs correspond to 1/25 of total proteins. GST-fusions were immunoblotted with GST antibodies. Rap1, ICAP-1 and H-Ras were immunoblotted with His-tag, ICAP-1 and H-Ras antibodies respectively. (B) GST-pull down of 1 μ M Rap1GTP γ S on 10 μ M GST-HypoKrit1 or 10 μ M GST-HypoKrit1 Δ C. Input corresponds to 1/4 of total Rap1. Rap1 was immunoblotted with His-tag antibody. These data are representative of four independent experiments.

Fig 4: Krit1, Rap1-GTP γ S and ICAP-1 form a ternary complex in vitro.

GST-pull-down of 5 μ M Krit1 or/and 5 μ M Rap1GTP γ S on 5 μ M GST-ICAP-1 fusion or GST alone. Krit1 binding to GST-ICAP-1 was visualized by Sypro Orange staining of the gel. Rap1 binding was visualized by western blot using His-tag antibody. These results were reproduced three times.

Fig 5: Rap1 binding to HypoKrit1 is not modified by Krit-Nter or ICAP-1.

(A) Comparaison by GST- pull down of the binding of 10 μ M Rap1GTP γ S to 3 μ M GST-HypoKrit1 in the absence or presence of 10 μ M Krit1-Nter and 10 μ M ICAP-1. Rap1 and Krit1-Nter were detected by immunoblotting using anti-His antibody. ICAP-1 was revealed by anti-ICAP-1 antibody. (B) FLAG-pull down of 3 μ M Rap1GTP γ S or 7 μ M GST-ICAP-1 to FLAG-Krit1 beads. Control corresponds to beads incubated with non transfected BHK cells and processed as FLAG-Krit beads. Input corresponds to 1/40 of total proteins. Proteins were stained by Sypro Orange.

These results are representative of three independent experiments.

(C) Model of the conformation of Krit1 in a binary complex with Rap1 or in a ternary complex with Rap1 and ICAP-1. Rap1 binds to the C-terminus of Krit1 closed and opened conformations. ICAP-1 binding opens Krit1 without perturbing Rap1 binding. For the clarity of the

representation only intramolecular folding has been represented. A head to tail intermolecular folding between two molecules of Krit1 is however not excluded.

Fig. 6. Krit1 interacts directly with microtubules in vitro via two sites in its N- and C-termini and Rap1 and ICAP-1 inhibits this interaction.

In each experiment, 40 pmoles of Krit1 were incubated in the absence or presence of taxol-stabilized MT polymerized in vitro from 150 pmoles of purified tubulin and centrifuged on sucrose gradient. Supernatant (S) and pellet (P) were analyzed by SDS-PAGE and the percentage of Krit1 bound to MT quantified by fluorometry. Krit1 precipitation in the absence of MT has been subtracted.

(A) Identification of MT binding sites on Krit1 using different Krit1 mutants. Arrowheads indicate Krit1 WT or mutants, T: Tubulin. Each experiment was repeated between two to four times.

(B) Inhibition of Krit1 binding to MT by Rap1 and ICAP-1. 200 pmoles of Rap1 or ICAP-1 were added to 40 pmoles of Krit1 and to polymerized MT. Each experiment was repeated three times.

Fig7. YFP-Krit1 co-localizes with CFP-labelled microtubules in transfected BHK cells and is delocalized by activated Rap1. BHK-cells were transfected with plasmids encoding YFP-Krit1 or YFP-ARNO and CFP-tubulin (A) together with pMT2HA-Rap1V12 (B) HA-Rap1V12 was detected with anti-HA 3F10 antibody. Scale bars: 15 μm .

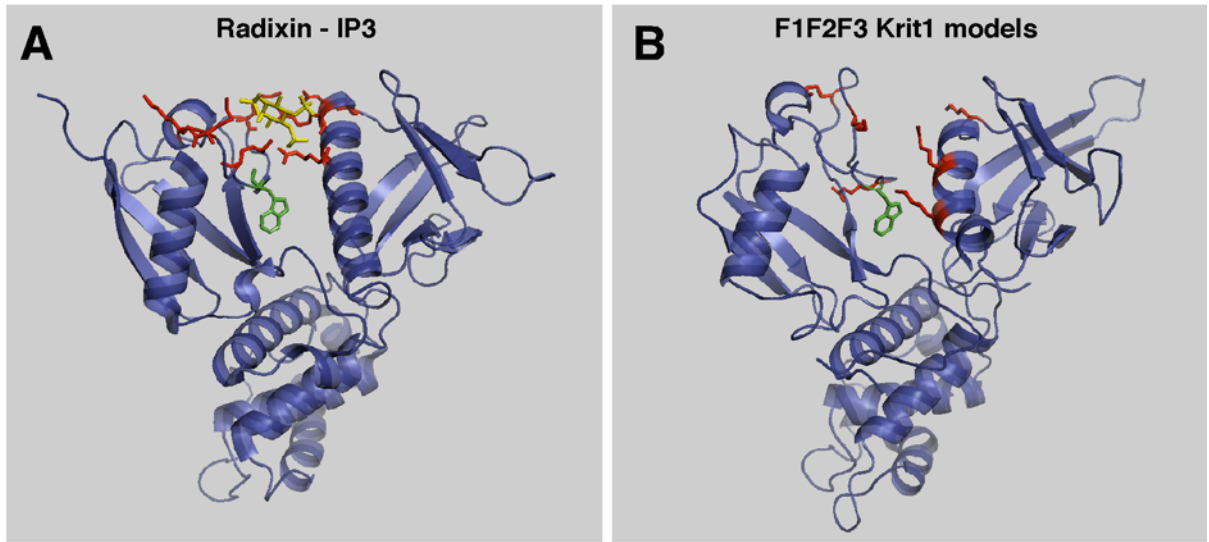
Fig. 8. Rap1 stimulates Krit1 binding to membranes.

(A) GST-HypoKrit1 (0.5 μM) was incubated with asolectin vesicles (1 mg/ml) in absence or presence of Rap1GTP γ S (3 μM). After centrifugation, the supernatant (S) and the pellet (P) were analyzed by SDS-PAGE and quantified by fluorometry. Protein precipitation in absence of liposomes has been subtracted. (B) Dose-response of stimulation of Krit1 binding to asolectin vesicles by increasing concentrations of Rap1GTP γ S. Each experiment was reproduced three times.

Fig 9. Model of regulation of Krit1 binding to microtubules and plasma membrane.

In the cell, Krit1 would be transported in its closed conformation along the microtubules toward the plasma membrane. When reaching the membrane, Krit1 would detach from MT and be captured by activated Rap1 and ICAP-1 on the plasma membrane.

Figure 1



C

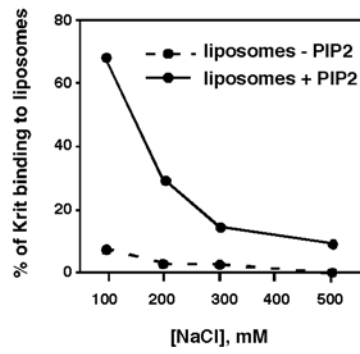
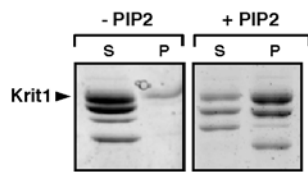


Figure 2

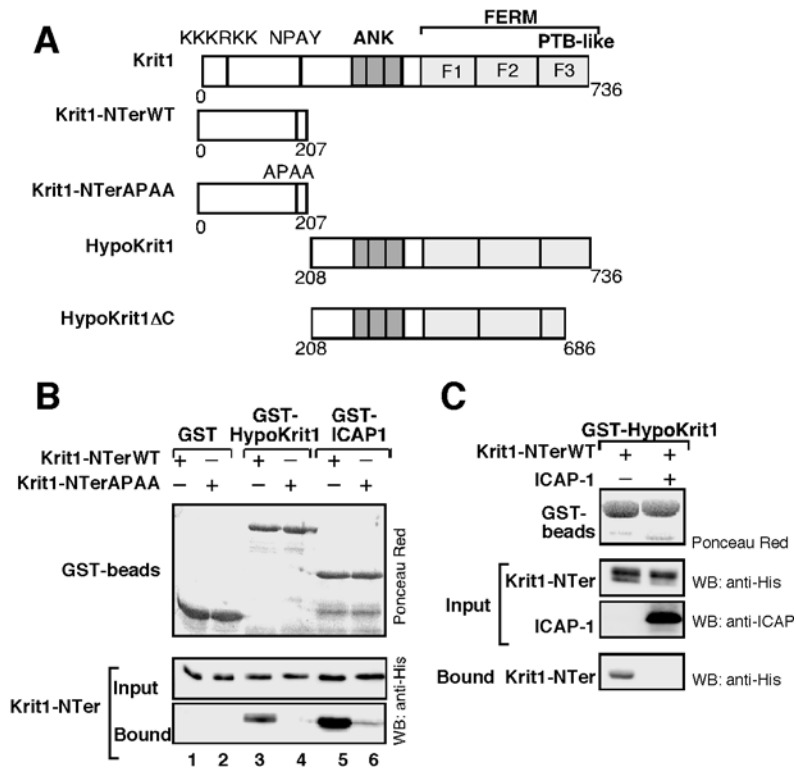


Figure 4

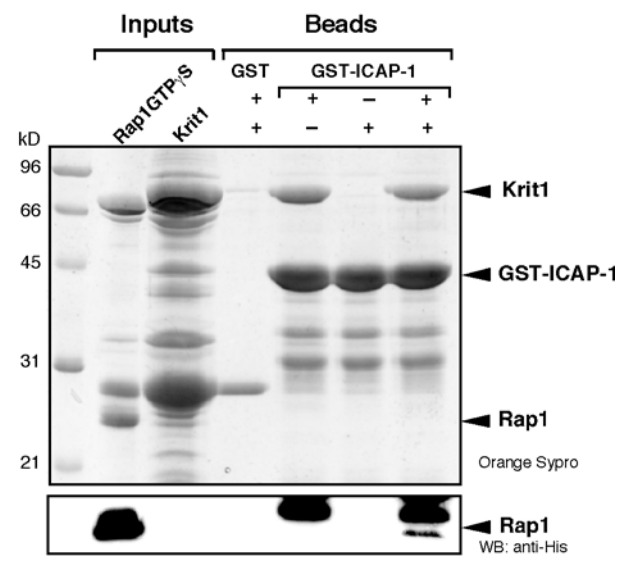


Figure 5

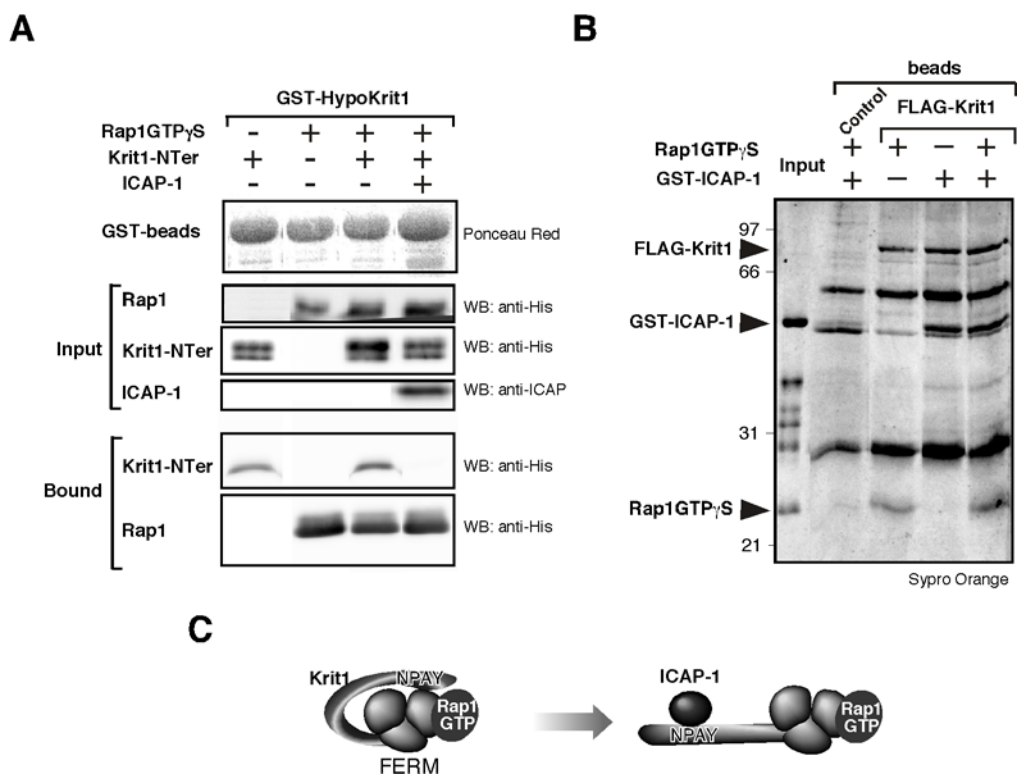
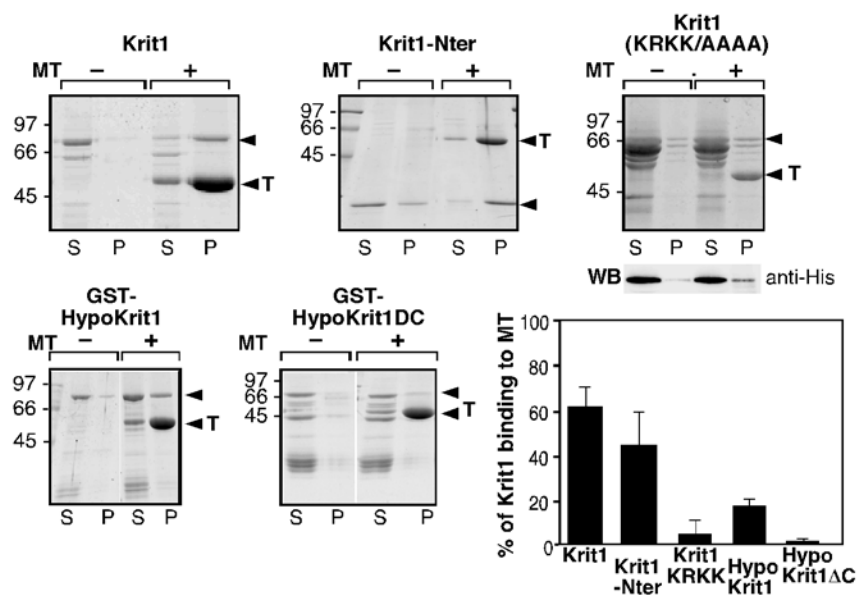


Figure 6

A



B

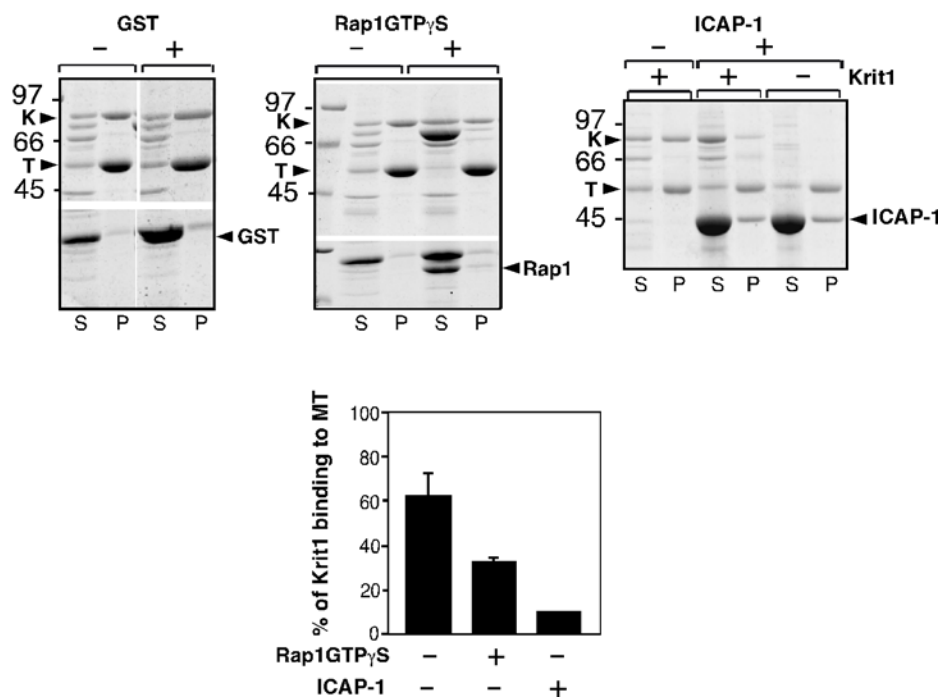
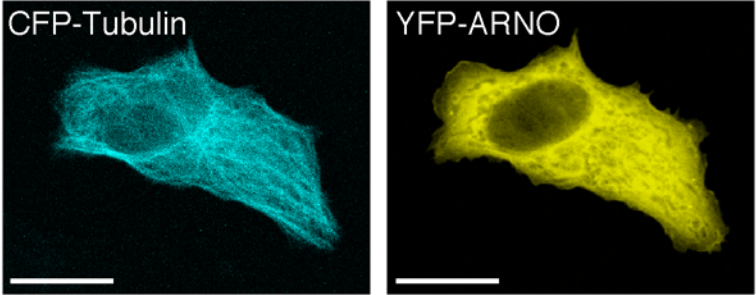


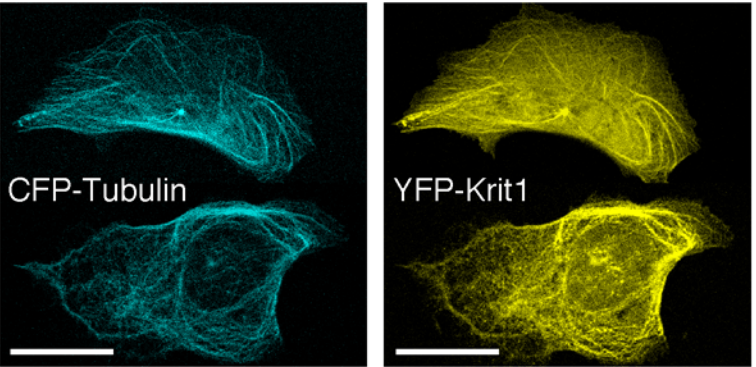
Figure 7

A

CFP-Tubulin + YFP-ARNO



CFP-Tubulin + YFP-Krit1



B

CFP-Tubulin + YFP-Krit1 + HA-Rap1V12

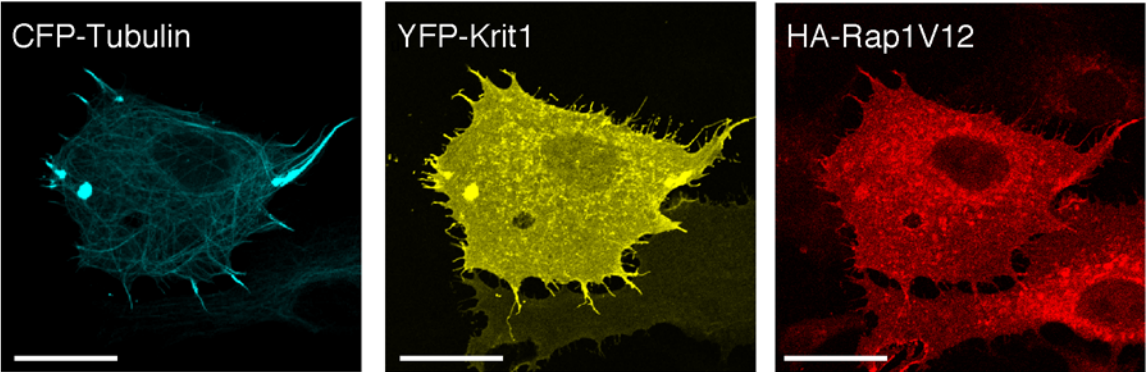


Figure 8

